Biomedicine & Pharmacotherapy 154 (2022) 113662

Contents lists available at ScienceDirect

Biomedicine & Pharmacotherapy

journal homepage: www.elsevier.com/locate/biopha

Perillaldehyde is a new ferroptosis inducer with a relevant clinical potential for acute myeloid leukemia therapy

Elena Catanzaro [a,b,1], Eleonora Turrini [c,1], Tessa Kerre [b,d,e,f], Simon Sioen [b,g], Ans Baeyens [b,g], Alessandra Guerrini [h], Mohamed Lamin Abdi Bellau [i], Gianni Sacchetti [h], Guglielmo Paganetto [h], Dmitri V. Krysko [a,b,j,2], Carmela Fimognari [c,*,2]

[a] Cell Death Investigation and Therapy (CDIT) Laboratory, Department of Human Structure and Repair, Ghent University, Corneel Heymanslaan 10, 9000 Ghent, Belgium
[b] Cancer Research Institute Ghent (CRIG), Ghent, Belgium
[c] Department for Life Quality Studies, University of Bologna, C.so d'Augusto 237, 47921 Rimini, Italy
[d] Department of Internal Medicine and Pediatrics, Ghent University, Corneel Heymanslaan 10, 9000 Ghent, Belgium
[e] Department of Diagnostic Sciences, Ghent University, Corneel Heymanslaan 10, 9000 Ghent, Belgium
[f] Department of Hematology, Ghent University Hospital, Corneel Heymanslaan 10, 9000 Ghent, Belgium
[g] Radiobiology Research Group, Department of Human Structure and Repair, Ghent University, Corneel Heymanslaan 10, 9000 Ghent, Belgium
[h] Pharmaceutical Biology Lab., Research Unit 7 of Terra&Acqua Tech Technopole Lab., Department of Life Sciences and Biotechnology, University of Ferrara, P.le Chiappini 2, 44123 Ferrara, Italy
[i] Sahrawi refugee camps, Tindouf, Algeria
[j] Department of Pathophysiology, Sechenov First Moscow State Medical University (Sechenov University), Bol'shaya Pirogovskaya Ulitsa, 19c1, Moscow 119146, Russia

ARTICLE INFO

Keywords:
Ammodaucus leucotrichus
R-perillaldehyde
Ferroptosis
ATP
Acute myeloid leukemia

ABSTRACT

Ferroptosis induction is an emerging strategy to treat cancer and contrast the tricky issue of chemoresistance, which can arise towards apoptosis. This work elucidates the anticancer mechanisms evoked by perillaldehyde, a monoterpenoid isolated from *Ammodaucus leucotrichus* Coss. & Dur. We investigated and characterized its antileukemic potential *in vitro*, disclosing its ability to trigger ferroptosis. Specifically, perillaldehyde induced lipid peroxidation, decreased glutathione peroxidase 4 protein expression, and depleted intracellular glutathione on HL-60 promyelocytic leukemia cells. Besides, it stimulated the active secretion of ATP, one of the most crucial events in the induction of efficient anticancer response, prompting further studies to disclose its possible nature as an immunogenic cell death inducer. To preliminarily assess the clinical relevance of perillaldehyde, we tested its ability to induce cell death on patient-derived acute myeloid leukemia biopsies, recording a similar mechanism of action and potency compared to HL-60 cells. To round the study off, we tested its selectivity towards tumor cells and disclosed lower toxicity on normal cells compared to both HL-60 and acute myeloid leukemia biopsies. Altogether, these data depict a favorable risk-benefit profile for perillaldehyde and reveal its peculiar antileukemic potential, which qualifies this natural product to proceed further through the drug development pipeline.

Abbreviations: 7-AAD, 7-aminoactinomycin D; *A. leucotrichus*, *Ammodaucus leucotrichus* Coss. & Dur; AML, acute myeloid leukemia; AMPK, AMP-activated protein kinase; DAMPs, damage-associated molecular patterns; DFO, deferoxamine; DMSO, dimethyl sulfoxide; DNTB, 5,50-dithiobis-(2-nitrobenzoic acid); ER, endoplasmic reticulum; GPX4, glutathione peroxidase 4; GSK, GSK2606414; EI, ionization energy; FBS, fetal bovine serum; fer-1, ferrostatin; G-CSF, granulocyte-colony stimulating factor; GM-CSF, granulocyte macrophage-colony stimulating factor; GSH, glutathione; GSSG, oxidized GSH; IC_{50}, inhibitory concentration causing 50% of cell toxicity; ICD, immunogenic cell death; IL-3, interleukin-3; MTT, 3-(4,5-dimethylthiazol-2-yl)-2,5-diphenyltetrazolium bromide; nec-1s, necrostatin-1s; PBMCs, peripheral blood mononuclear cells; PE, phycoerythrin; PERK, PKR-like endoplasmic reticulum kinase; PI3K, phosphoinositide 3-kinase; PS, phosphatidylserine; RIPK, receptor-interacting protein kinase; RANKL, receptor activator of NF-κB ligand; ROS, reactive oxygen species; SCF, stem cell factor; vit-E, vitamin E; zVAD-fmk, carbobenzoxy-valylalanyl-aspartyl-[O-methyl]-fluoromethylketone.

* Corresponding author.
E-mail address: carmela.fimognari@unibo.it (C. Fimognari).
[1] These authors contributed equally to this work.
[2] These authors shared senior authorship.

https://doi.org/10.1016/j.biopha.2022.113662
Received 11 July 2022; Received in revised form 1 September 2022; Accepted 1 September 2022
Available online 7 September 2022

1. Introduction

Programmed cell death is a crucial event for the maintenance of homeostasis, normal development, and the prevention of hyperproliferative diseases such as cancer [1]. If apoptosis has been accounted as the only regulated form of cell death for a long time, nowadays more than 12 types of regulated cell death modalities have been discovered [2]. Anticancer treatment has long been based on compounds promoting apoptosis, but apoptosis evasion represents a mechanism for cancer cells to survive and a way to develop anticancer drugs' resistance [3]. Thereby, the other well recognized forms of regulated cell death represent a promising strategy to eradicate tumors efficiently and overcome resistance [4]. Necroptosis and ferroptosis, for instance, represent two concrete alternatives to apoptosis in fighting different tumor types. Necroptosis is one of the most studied form of regulated necrosis, executed by receptor-interacting protein kinase (RIPK)-1, RIPK-3, and mixed lineage kinase domain-like pseudo-kinase [5]. Ferroptosis, on the other hand, is an iron-dependent cell death program characterized precisely 10 years ago, which plays a pivotal role in suppressing cancer growth and progression [6]. Basically, dysfunction in iron and lipid metabolism provokes the accumulation of reactive oxygen species (ROS) and lipid peroxidation, resulting in cell death. The accumulation of lipid ROS is due to the inability of ferroptotic cells to quench the reactive species as result of glutathione peroxidase 4 (GPX4) inoperability. Physiologically, GPX4 reduces hydrogen peroxide or organic hydroperoxide to water or the corresponding alcohols by converting glutathione (GSH) to oxidized GSH (GSSG). Thus, the inhibition of GPX4 leads to the accumulation of lipid ROS and triggers the ferroptotic cell death cascade. GPX4 can be inhibited directly, or its activity can be blocked, for instance, by making GSH unavailable. The inhibition of the amino acid anti-port Xc- system is an example of the latter event. This system is responsible for the intracellular transport of extracellular cystine, which is exchanged for intracellular glutamate. Once inside the cell, cystine is reduced to cysteine, an essential substrate for synthesizing GSH. Consequently, inhibition of the Xc- system alters the biosynthesis of GSH and impedes the antioxidant activity of GPX4 [6,7].

The natural world is one of the primary sources of anticancer agents. Indeed, over 50% of current chemotherapeutic drugs belongs to natural compounds [8,9], and, interestingly, some of them trigger non-apoptotic mechanisms of regulated cell death [10]. *Ammodaucus leucotrichus* Coss. & Dur (*A. leucotrichus*), commonly known as "hairy cumin", is a medicinal plant belonging to the family *Apiaceae* that grows in the Saharan and Sub-Saharan countries. A wide range of traditional medicinal uses is reported for this plant. It has been used in decoctions or infusion to treat cardiac diseases, digestive problems, diabetes, or for its aphrodisiac and tonic properties [11]. The fruit extracts or oils from *A. leucotrichus* exhibit many biological and pharmacological activities such as antioxidant, antibacterial, anti-inflammatory, and neuroprotective [11]. The phytochemical characterization of the plant identified several bioactive chemical constituents, including terpenes, tannins, anthracene compounds, sterols, reducing compounds, *etc.* Perillaldehyde, a natural monoterpenoid agent, is one of the main components of *A. leucotrichus* [12–15], with the absolute configuration of S-(-)-perillaldehyde as reported by Khalfaoui et al. [16]. It exhibits anti-inflammatory, antioxidant, and antifungal activity. Of interest that it is currently used to maintain the quality and safety of food and is used in cosmetics perfumery and pharmaceutical industry [17–19]. Previous data reported the *in vitro* antiproliferative and cytotoxic activity of perillaldehyde on human alveolar basal epithelial adenocarcinoma A549 cells, but the molecular mechanism of action has not been fully investigated [20]. Besides, perillaldehyde suppressed cell proliferation in mouse and human gastric cancer cells through activation of AMPK (AMP-activated protein kinase), responsible for the initiation of autophagy [21]. Moreover, in prostate cancer cells, perillaldehyde shows antimetastatic activity by inhibiting bone metastasis through the repression of the receptor activator of NF-κB ligand (RANKL) [22]. Overall, the potential anticancer activity of perillaldehyde was that promising to prompt also the design, synthesis, and investigation of different analogues, such as amino-modified derivatives of (S)-perillyl alcohol or its epoxides which both demonstrated an interesting cytotoxic effects on different tumor models [18,23–26].

In the present paper, we extensively elucidate the anticancer mechanisms evoked by perillaldehyde, investigating, and characterizing its antileukemic potential *in vitro* and preliminarily assessing its clinical potential. To reach the latter aim, we tested the selectivity of perillaldehyde towards malignant cell lines and its efficiency in killing primary acute myeloid leukemia (AML) samples.

2. Materials and methods

2.1. Reagents

RPMI 1640, DMEM high glucose, heat inactivated fetal bovine serum (FBS), 1% L-glutamine solution 200 mM and 1% penicillin (10.000 units)/streptomycin (10 mg/mL) solution were all obtained from Gibco (Life Technologies, Monza, Italy).

Guava Viacount reagent and Guava Nexin reagent were purchased by Luminex (Austin, TX, USA).

The antibodies anti-GPX4 (no. PA5–109274) and anti-rabbit secondary antibody (no. A21244) were provided by Invitrogen (Thermo Fisher Scientific, Waltham, MA, USA). Cell Lytic™, 3-(4,5-dimethylthiazol-2-yl)-2,5-diphenyltetrazolium bromide (MTT), Ellman's Reagent [5,50-dithiobis-(2-nitrobenzoic acid) or DNTB], trichloroacetic acid, TRIS-EDTA, formaldehyde, methanol, necrostatin-1s (nec-1s), deferoxamine (DFO), vitamin E (vit-E) were all purchased from Merck (Darmstadt, Germany). Bradford assay was provided by Bio-Rad (Basel, Switzerland).

Sytox Green, Sytox Blue, BODIPY 581/591 C11 were provided by Thermo Fisher Scientific and CellTiter-Glo® Luminescent Cell Viability Assay by Promega (Madison, WI, USA). Carbobenzoxy-valylalanyl-aspartyl-[O-methyl]-fluoromethylketone (zVAD-fmk) was purchased by Bachem (Bubendorf, Switzerland), and ferrostatin-1 (fer-1) by Calbiochem (San Diego, CA, USA). The inhibitors olaparib, GSK2606414 (GSK), wortmannin, and brefeldin A were all provided by Selleckchem (Houston, TX, USA).

2.2. Phytochemical characterization

2.2.1. Plant material

The fruits of *Ammodaucus leucotrichus* L. were collected from wild population of plants at Bir Lehlu (coordinates: 26°20'58"N 09°34'32"W, Western Sahara) in march 2016. Plant material collection was carefully performed in order not to damage the wild population and obtaining a representative sample from no less than 10 plants. The samples authentication was performed by dr. Mohamed Lamin Abdi Bellau and prof. Alessandra Guerrini, according to IUCN Centre For Mediterranean Cooperation (2005). Plant material was dried at room temperature for 15 days.

2.2.2. Hydro-distillation of essential oil

The pale green essential oil, with a characteristic odor, was obtained by hydro-distillation of 20 g of dried fruits, using 500 mL of water in a Clevenger-type apparatus for 3 h. The obtained essential oil was pooled separately, dried over anhydrous sodium sulfate (Na_2SO_4), and stored at 4 °C in amber glass vials until analysis.

2.2.3. Isolation and characterization of perillaldehyde

Flash chromatography was performed on silica gel (Silica gel 60 mesh, particle size: 0.035–0.070 mm) from essential oil. The column (height: 30 cm; diameter: 4.5 cm) was prepared by wet method. The essential oil was loaded into the column head and dissolved in the minimum mobile phase volume. The eluent system used was hexane:

ethyl acetate mixture at 80:20 v:v ratio. The pure fraction of perillaldehyde was identified through TLC (silica gel 60 F254; thickness 0.25 mm; Merck), visualized at 254 nm and 366 nm, and finally developed with a solution of 1 g of phosphomolybdic acid in 10 mL of ethanol.

GC-MS was used to analyze the identity and the purity of the separated molecule. The GC-MS analysis was performed with a Varian 3800 chromatograph (Varian, Palo Alto, CA, USA) equipped with a Varian Factor Four VF-5 ms column (5%-phenyl-95%-dimethylpolysiloxane, internal diameter: 0.25 mm, length: 30 m) interconnected with a Varian mass spectrometer SATURN MS-4000 (Varian), with electronic impact ionization, ion trap analyzer and software provided with the NIST database for the identification of components. The experimental conditions used were the following: helium carrier gas (1 mL/min), split ratio of 1:50, ionization energy (EI) 70 eV, emission current of 10 μA, scan rate of 1 scan/sec, mass range 40–400 Da. For the analysis, the oven initial temperature of 70 °C was increased to 230 °C with a rate of 4 °C/min and maintained at 230 °C for 10 min; finally, it was brought from 230° to 280°C with an increase of 5 °C/min. The total time of acquisition of the chromatogram was 70 min. The arithmetic index of perillaldehyde was determined adding a C_8–C_{32} *n*-alkanes (Sigma-Aldrich, St. Louis, MO, USA) mixture to the essential oil before injecting in the GC–MS equipment, following the same conditions reported above.

The pure perillaldehyde was compared with the commercial S-(-)-perillaldehyde (Sigma-Aldrich) through GC analyses, performed with a Thermo Focus-gas chromatograph equipped with a flame ionization detector and a chiral Megadex 5 column (25 m × 0.25 mm), with the following temperature program: 80–200 °C, rate 2 °C min^{-1}. Optical rotation was measured at 20 ± 2 °C in ethanol, 10% concentration; $[\alpha]_D^{20}{}_D$ value is given in $10^{-1}degcm^2g^{-1}$.

2.3. Cell lines and cell cultures

2.3.1. Cell lines

Human acute T leukemia cells (Jurkat), human colon adenocarcinoma cells (DLD-1), and human neuroblastoma cells (SHSY5Y) were purchased from LGC Standard (LGC Group, Middelsex, UK); human promyelocytic leukemia cells (HL-60) were obtained from Istituto Zooprofilattico of Brescia (Italy). Jurkat and DLD-1 were propagated in RPMI 1640 supplemented with 10% FBS, 1% L-glutamine solution and 1% penicillin/streptomycin solution. HL-60 were cultured in the same culture medium with the only exception of 20% inactivated FBS and, to avoid spontaneous differentiation, cell density was never allowed to exceed 1.0×10^6 cells/mL. SHSY5Y were propagated in DMEM high glucose supplemented with 10% FBS, 1% L-glutamine and 1% penicillin/streptomycin. All cells were incubated at 37 °C with 5% CO_2 in humified atmosphere.

2.3.2. Peripheral blood monocytes and primary AML samples

Peripheral blood samples were collected by venipuncture from volunteers in lithium-heparinized tubes at Ghent University Hospital (UZ Gent). Informed consent for inclusion was received from all volunteers before participating in the study (Reference no. 2019–0461). Peripheral blood mononuclear cells (PBMCs) were isolated using density-gradient centrifugation (Lymphoprep). The cell viability and yield of the isolated PBMCs were verified with Türk (Gibco, Thermo Fisher Scientific Ltd., Waltham, MA, USA). PBMC culture medium consisted of RPMI with antibiotics (50 U/mL penicillin and 50 mg/mL streptomycin, Gibco), supplemented with 10% FCS at 37 °C.

AML samples (leukapheresis of hyperleucocytic patients) have been provided by prof. dr. Tessa Kerre. Leukapheresis samples from patients were prepared by Ficoll separation (Lymphoprep, Nycomed Pharma, Brussels, Belgium) and cryopreserved in fetal calf serum (FCS, Gibco, Invitrogen, Merelbeke, Belgium) containing 10% dimethyl sulfoxide (DMSO, Serva, Heidelberg, Germany) in liquid nitrogen. After thawing, samples were cultured in standard medium supplemented with 50 ng/mL interleukin-3 (IL-3, PeproTech, London, UK), 100 ng/mL granulocyte macrophage-colony stimulating factor (GM-CSF, VIB protein core, Ghent, Belgium), 100 ng/mL granulocyte-colony stimulating factor (G-CSF, PeproTech), and 25 ng/mL stem cell factor (SCF, PeproTech). Cell viability was monitored daily. Samples were obtained following the guidelines of the Medical Ethical Committee of Ghent University Hospital, after informed consent had been obtained in accordance with the Declaration of Helsinki.

2.4. Cell viability assay

SHSY5Y, DLD-1, Jurkat and HL-60 cells were treated with increasing concentration of perillaldehyde (0.05 – 0.60 mM) for 24 h or shorter time according to experimental exigencies. The analysis of cell viability was performed using two different tests: a cell membrane permeability test with Guava ViaCount Reagent containing 7-aminoactinomycin D (7-AAD) was used for suspension cells (Jurkat, HL-60) and the metabolic MTT assay for adherent cells (SHSY5Y, DLD-1). The inhibitory concentration causing 50% of cell toxicity (IC_{50}) following one cell-cycle exposure was calculated by interpolation from a dose-response curve.

The analysis of cell death of HL-60 and Jurkat cells was performed using specific inhibitors and the cell-impermeant fluorescent nuclear probe Sytox Green as previously described in [27]. In brief, cells were pre-treated for 1 h with or without the pan-caspase inhibitor zVAD-fmk (50 μM) or the PARP inhibitor olaparib (2 μM), which block apoptosis; the RIPK1 inhibitor nec-1s (20 μM), which blocks necroptosis; the iron chelator DFO (10 μM), the inhibitors of ROS vit-E (100 μM) or fer-1 (1 μM) that also inhibits lipid peroxidation, all three responsible for the inhibition of ferroptosis. Then, cells were treated for 24 h with perillaldehyde and viability was analyzed *via* flow cytometry.

To analyze cell death in PBMCs, cells were seeded in a 96-well plate at a cell concentration of 500,000 cells/mL. PBMCs were treated with increasing concentrations of perillaldehyde (0.075–2.4 mM). Cell death was assessed at 0, 24 and 48 h after addition. We analyzed cell death as an increase in fluorescence intensity of the cell-impermeable dye (Sytox Green) after plasma membrane disintegration. Fluorescence was measured on a Tecan Spark 20 M multimode microplate reader (Tecan, Männedorf, Switzerland).

The analysis of cell death on AML samples was performed flow cytometrically on LSR II Fortessa using Sytox Blue as viability dye and the same inhibitors concentration and treatment protocol used for HL-60 cells.

2.5. Annexin-V assay

After 24 h treatment, cells were incubated with 100 μL of Guava Nexin Reagent, containing 7-AAD and annexin V-phycoerythrin (PE), for 20 min at room temperature in the dark. After incubation, cells were analyzed by flow cytometry.

2.6. Measurement of lipid ROS

To measure lipid ROS, the fluorescent BODIPY 581/591 C11 has been exploited. BODIPY 581/591 C11 has an intrinsic red fluorescent. After the interaction with peroxyl radicals, its chemical structure changes and the fluorescence shifts in the green channel. To monitor lipid oxidative stress, we treated HL-60 cells with perillaldehyde 0.30 mM or RSL3 0.5 μM for different time points in a medium containing 2% FBS. Then, cells were washed and stained for 30 min at 37 °C in FBS-free medium containing 0.5 μM BODIPY 581/591 C11. Cells were then washed and resuspended in a solution of Sytox Blue 3 μM used as a viability dye. After 10 min, the samples were analyzed by a BD FACSCanto flow cytometer. As gating strategy, dead cells (Sytox Blue positive) were excluded, and green fluorescence increase was used as an indicator of cells characterized by lipid oxidative stress.

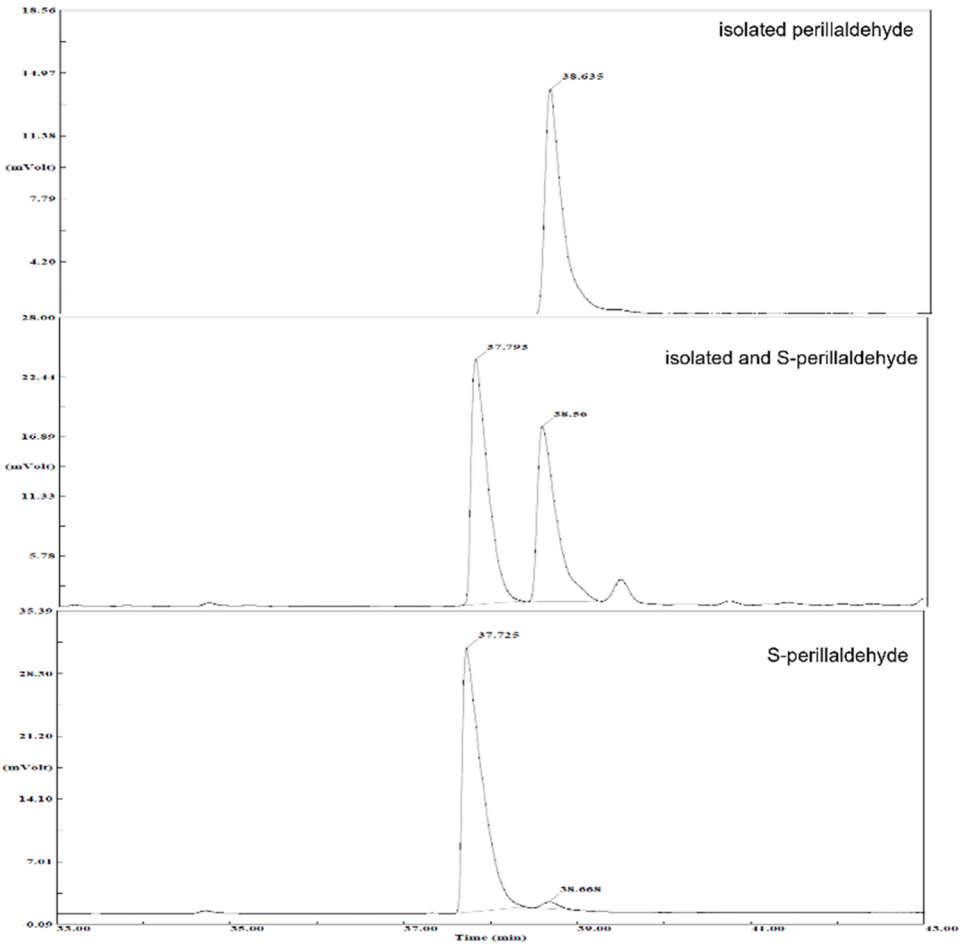

Fig. 1. Perillaldehyde R-enantiomer is the main component isolated from *A. leucotrichus* essential oil. (a) Chromatogram and retention time (38.635 min) of perillaldehyde enantiomer isolated from *A. leucotrichus*. **(b)** Chromatogram and retention time of the mixture of commercial (S-enantiomer) and isolated perillaldehyde (37.793 min and 38.56 min, respectively). **(c)** Chromatogram and retention time of S-perillaldehyde (37.725 min). GC-FID analyses were performed with chiral column.

2.7. Analysis of GPX4 expression

GPX4 expression was determined 6 or 24 h after treatment of HL-60 cells with increasing concentrations of perillaldehyde. Briefly, 10^6 cells of each sample were fixed with 4% formaldehyde and permeabilized using 90% cold methanol. Samples were washed with incubation buffer (1x PBS + 1% bovine serum albumin) and incubated for 1 h at 4 °C with the primary antibody anti-GPX4 (1:150). After washing, cells were incubated with the anti-rabbit secondary antibody (1:200) for 1 h at 4 °C. Cells were then washed and analyzed by flow cytometry. Results are expressed as fold change of mean fluorescence intensity of treated cells compared to untreated cells.

2.8. Measurement of reduced GSH

Ellman's reagent (DNTB) was used to measure the intracellular level of GSH in HL-60 cells. Briefly, after treatment with perillaldehyde cells were lysed using Cell Lytic™ reagent. The supernatant containing cytoplasmic proteins was collected and protein content measured by the Bradford assay. An equal protein amount for each sample was used to quantify GSH content. Samples were mixed with trichloroacetic acid and centrifuged at 14,000 rounds for 5 min to remove precipitated proteins. 50 μL of supernatant was added to TRIS-EDTA (pH 8.9; 0.2 M) and mixed to DTNB (0.01 M in methanol). DNTB reacts with GSH, producing 2-nitro-5-thiobenzoic acid and GSH disulfide, a yellow-colored product [28]. The spectrophotometric analysis was performed at 405 nm within 5 min with the microplate reader Infinite F200 PRO (Tecan). Results are expressed as fold change of treated cells compared to untreated ones.

2.9. Measurement of intracellular and extracellular ATP levels

CellTiter-Glo® Luminescent Cell Viability Assay was used to measure intracellular and extracellular ATP levels [29]. HL-60 has been treated with perillaldehyde for different time points in medium containing 2% of FBS. Then, cells were pelleted and transferred to a white 96-well plate. Contextually, the supernatants were transferred to another white 96-well plate. The assay was performed following the manufacturer instructions. 100 μL of reconstituted reagent was added to cells or to 100 μL of supernatant. Cells were mixed in an orbital shaker for 2 min and then incubated at room temperature for 10 min. Luminescence was measured with the Tecan Spark 20 M multimode microplate reader. ATP has been expressed as a fold increase compared to untreated cells.

For the experiments with the inhibitors, cells were pretreated for 1 h with or without wortmannin (0.2 μM), GSK (0.1 μM) or brefeldin A (0.1 μM). Then, cells were treated for 3 h with perillaldehyde, and ATP analysis was performed as above.

2.10. Flow cytometry

The flow cytometric analyses were performed with Guava EasyCyte 6–2 L (Merck) or FACSCanto cytometer (Becton Dickinson, BD, San Jose, CA, USA). At least 10,000 events were recorded for each sample. In all the analyses debris and clumps were gated out.

2.11. Statistical analysis

All experiments were performed at least in triplicate and results are expressed as mean ± SEM. Differences among treatment were analyzed

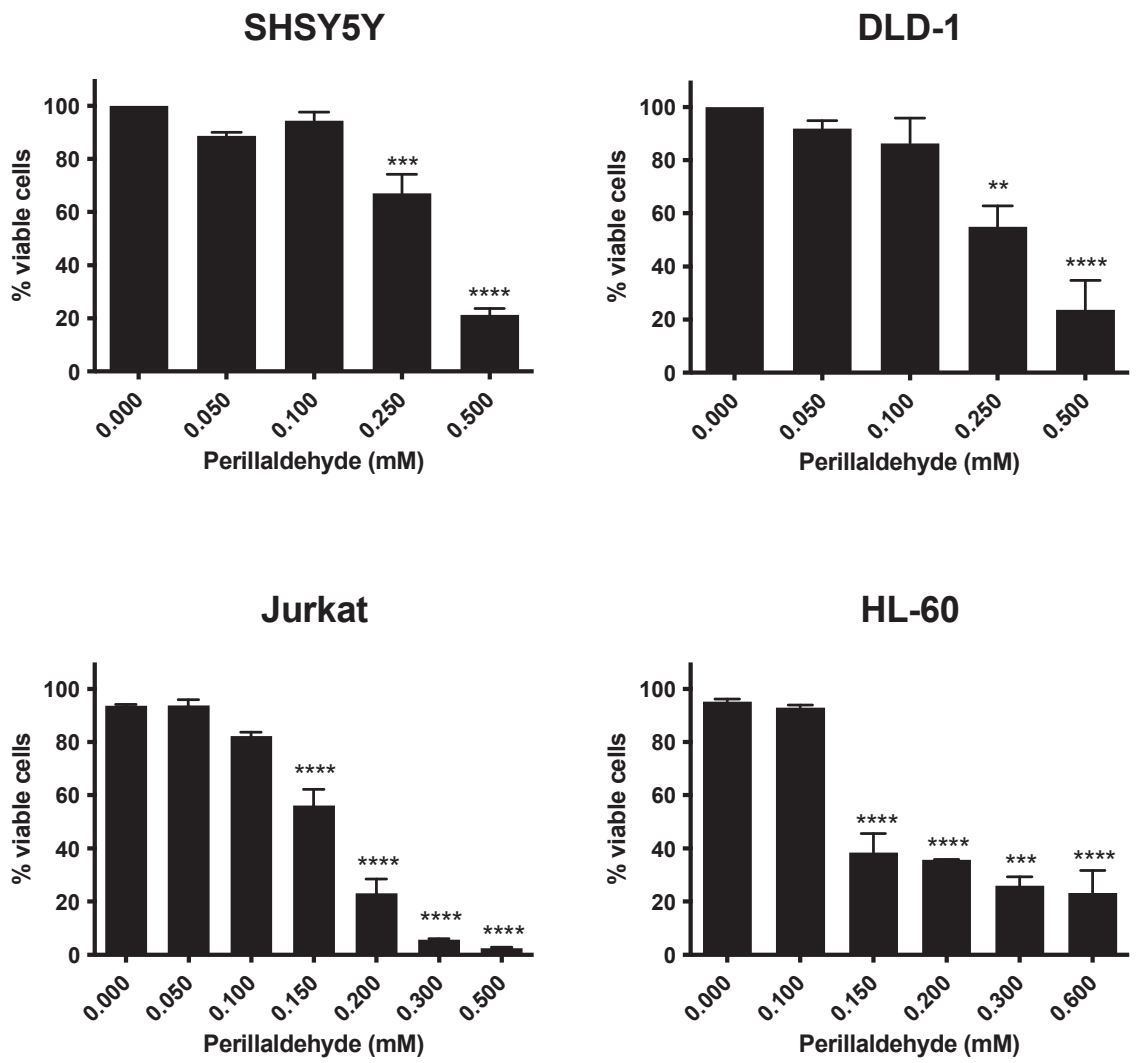

Fig. 2. Perillaldehyde decreased cell viability in a concentration-dependent fashion in all analyzed cell lines. Cytotoxic effects of perillaldehyde after 24 h treatment of SHSY5Y, DLD-1, Jurkat and HL-60 cells. Cell death was analyzed using MTT test for SHSY5Y and DLD-1, whereas a cell membrane permeability test was used for Jurkat and HL-60 cells. Statistical significance was calculated by one-way Anova followed by Dunnet's multiple comparisons test. * * $p < 0.01$; * ** $p < 0.001$; * ** * $p < 0.0001$ compared to untreated cells.

using repeated Anova, followed by Bonferroni, Dunnet or Uncorrected Fisher's LSD as post- test, using GraphPad InStat version 6.00 (GraphPad Prism, San Diego, CA, USA). $p < 0.05$ was considered significant. The IC_{50} was calculated by interpolation from the non-linear dose-response curve.

3. Results and discussion

3.1. Perillaldehyde is the main component of A. leucotrichus essential oil

The GC-MS of *A. leucotrichus* essential oil highlighted perillaldehyde as the main component, with an experimental arithmetic index of 1269, comparable to the literature value of 1272 as well as the experimental mass fragmentation (*m/z*): 151 (15), 150 (15), 135 (50), 122 (45), 107 (70), 93 (60), 91 (75), 79 (100), 68 (55), 67 (100), 77 (45), 53 (30) [30]. The optical rotation was: $[\alpha]_D^{20} = +115$ (c 10, ethanol), opposite to the commercial S-(-)-perillaldehyde. The injection of both enantiomers in GC-FID, equipped with chiral column, confirmed that the isolated perillaldehyde is not superimposable with the commercial one and corresponded to the R enantiomer (Fig. 1), in contrast to previous literature [16], where the authors probably supposed the absolute configuration, but they have not shown experimental evidences.

Table 1
IC_{50} values calculated after 24 h of treatment with increasing concentrations of perillaldehyde.

Cell line	IC_{50} (mM)
Human neuroblastoma cells (SHSY5Y)	0.257
Human colon adenocarcinoma cells (DLD-1)	0.273
Human acute T leukemia cells (Jurkat)	0.162
Human promyelocytic leukemia cells (HL-60)	0.129

3.2. Perillaldehyde induces ferroptosis in vitro

We tested perillaldehyde on a panel of cancer cell lines (*i.e.*, SHSY5Y, DLD-1, Jurkat, and HL-60), representing both solid and hematological tumors. Cells' sensitivity was assessed based on the half maximal inhibitory concentration (IC_{50}) values calculated after 24 h from treatment (Fig. 2 and Table 1). The HL-60 promyelocytic leukemia cells resulted the most sensitive to perillaldehyde treatment and, for this reason, the investigation on the mechanisms underpinning its cytotoxic effects has been investigated in that cell line.

To understand whether perillaldehyde induces a regulated form of cell death and to better understand the stage of cell death, we performed

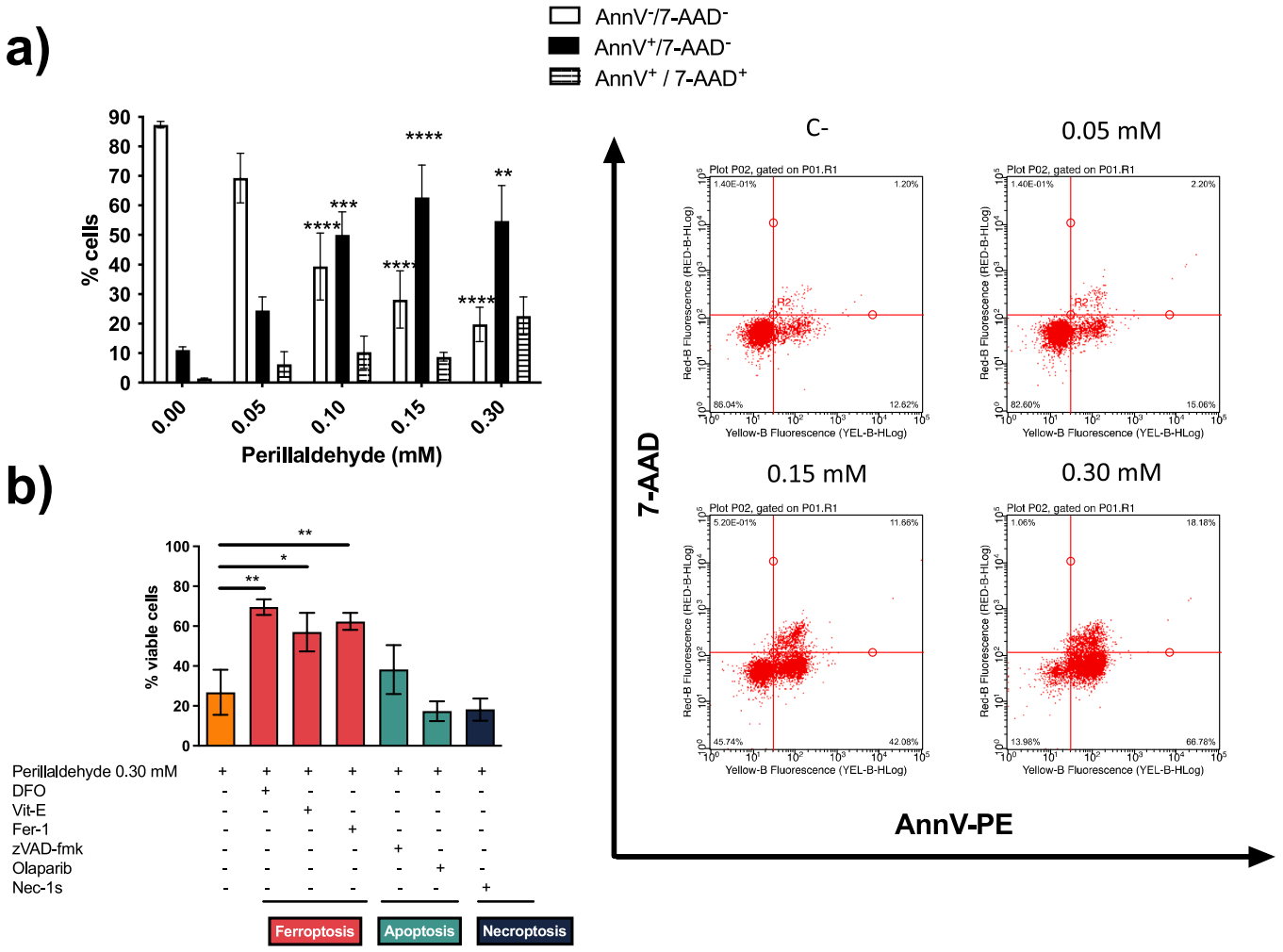

Fig. 3. Perillaldehyde induces ferroptosis in acute myeloid leukemia HL-60 cell line. (**a**) Percentage and representative dot plots of Annexin-V$^-$/7-AAD$^-$, Annexin-V$^+$/7-AAD$^-$, Annexin-V$^+$/7-AAD$^+$ HL-60 cells after 24 h treatment with perillaldehyde. Experiments performed on HL-60 cells treated with perillaldehyde demonstrated that regulated mechanisms of cell death are triggered by perillaldehyde, as indicated by PS exposure. Statistical significance was calculated by two-way Anova followed by Dunnet's multiple comparisons test. * * $p < 0.01$; * ** $p < 0.001$; * ** * $p < 0.0001$ compared to the equivalent population of untreated cells. (**b**) % of viable cells after 1 h pre-treatment with inhibitors and treatment for 24 h with perillaldehyde 0.30 mM. Sytox Green was used as viability dye. Only inhibitors of ferroptosis were able to block cell death, while inhibitors of apoptosis and necroptosis were ineffective. The following concentrations of inhibitors were used: 25 μM zVAD-fmk, 2 μM olaparib, 20 μM nec-1s, 1 μM fer-1, 10 μM DFO and 100 μM vit-E. Statistical significance was calculated by one-way Anova followed by Dunnet's multiple comparisons test. * $p < 0.05$; * * $p < 0.01$ compared to cells treated with perillaldehyde.

the annexin-V assay. One of the earliest events in most regulated cell deaths, such as apoptosis or necroptosis, is the externalization of phosphatidylserine (PS), which is normally restricted to the inner leaflet of the phospholipidic membrane [31]. The exposure of PS was assessed on HL-60 cells by its affinity for the phospholipid binding protein annexin-V. To differentiate cells undergoing early cell death from late cell death, the viability dye 7-AAD was used as marker of membrane integrity. The flow cytometric analysis with 7-AAD and annexin-V allows to identify cells in the early cell death stage (Annexin-V$^+$/7-AAD$^-$) or late cell death stage (Annexin-V$^+$/7-AAD$^+$). An increase in the fraction of annexin-V$^+$/7-AAD$^-$ cells was recorded starting from the concentration 0.10 mM (50% of treated cells compared to 11% in untreated cells) (Fig. 3**a**). At the highest concentrations tested, the percentage further increased to 70% of annexin-V$^+$/7-AAD$^-$ cells (Fig. 3**a**), confirming the ability of perillaldehyde to kill tumor cells in a regulated fashion.

Since PS exposure occurs in different types of regulated cell death [31–33], to characterize the modalities of death triggered by perillaldehyde, specific inhibitors of apoptosis, necroptosis and ferroptosis were used. All inhibitors of ferroptosis significantly rescued HL-60 cells after 24 h perillaldehyde exposure (Fig. 3**b**). In particular, perillaldehyde's cytotoxic potential was antagonized by the iron chelator DFO and both lipidic ROS scavengers vit-E and fer-1, envisaging these compounds as promising ferroptosis inducers. However, neither nec-1s nor apoptosis's inhibitors (*i.e.,* zVAD-fmk and olaparib) significantly counteracted perillaldehyde's cytotoxic effects (Fig. 3**b**), suggesting that perillaldehyde induces cell death by triggering ferroptosis.

To check whether the mechanism of action was cell line-dependent, we performed the same experiments in a different cell line. The ability of perillaldehyde to trigger ferroptosis was also recorded on the Jurkat acute T-cell leukemia cells. Annexin-V/7-AAD assay and the experiment with inhibitors confirmed ferroptosis as the main form of cell death triggered by perillaldehyde (Fig. S1).

These results prompted us to explore the key events leading to

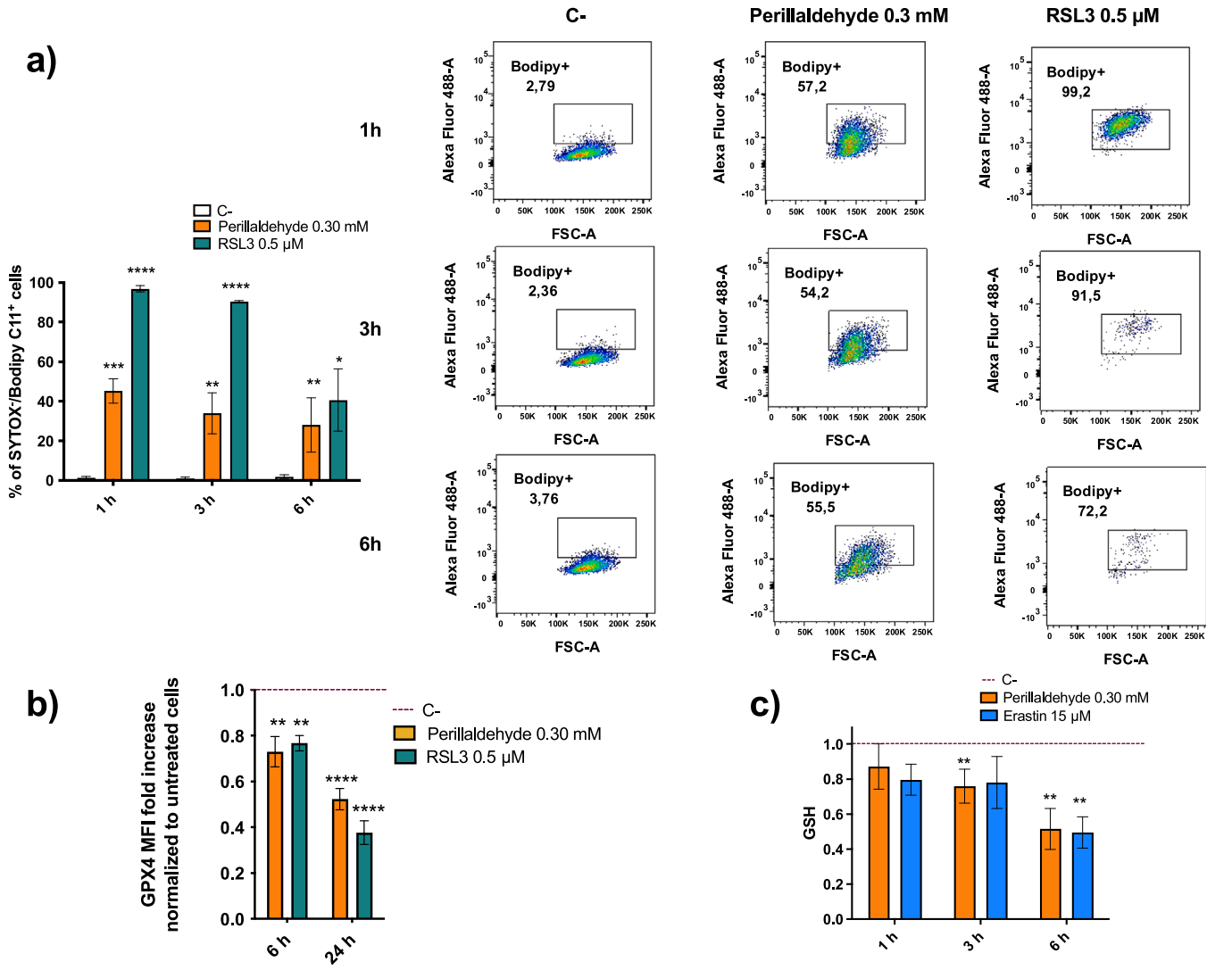

Fig. 4. Perillaldehyde significantly increases intracellular lipid ROS and decreases GPX4 and GSH levels in acute myeloid leukemia HL-60 cell line. (**a**) % of Sytox Blue^{-}/C11-BODIPY^{+} HL-60 cells after 1, 3, and 6 h of treatment with perillaldehyde 0.30 mM. 0.5 µM RSL3 was used as positive control. (**b**) Protein expression of GPX4, expressed as fold change of treated cells *versus* untreated ones. Cells were treated with perillaldehyde 0.30 mM or RSL3 0.5 µM for 6 and 24 h. (c) Intracellular GSH content, expressed as fold change of treated cells *versus* untreated ones. Cells were treated with perillaldehyde 0.30 mM or erastin 15 µM for 1, 3, and 6 h. Statistical significance was calculated by two-way Anova followed by Dunnet's multiple comparisons test. * $p < 0.05$; * * $p < 0.01$; * ** $p < 0.001$; * *** * $p < 0.0001$ compared to untreated cells.

ferroptotic cell death after perillaldehyde treatment.

3.3. *Perillaldehyde triggered the main key events of ferroptosis*

To confirm and characterize the molecular mechanisms underlying perillaldehyde-induced ferroptosis, we investigated the modulation of some of the most significant markers and events required for the execution of this regulated cell death: lipid oxidative stress induction, modulation of GPX4 expression and intracellular GSH content.

Despite the mechanism of action, all ferroptosis inducers converge in the common priming effect, which is triggering oxidative lipid stress. The increase in lipid ROS is an early event during ferroptosis [34]. In our experimental setting, the flux of lipid ROS in cell membranes was monitored after 1, 3, and 6 h from perillaldehyde treatment of HL-60 cells using C11-BODIPY. A significant increase in lipid ROS was recorded starting from 1 h of treatment, with 50% of viable cells (cells negative to the Sytox Blue staining) positive for C11-BODIPY (Fig. 4**a**). RSL3, used as a positive control, induced an analogous time-dependent trend in promoting lipid oxidative stress (Fig. 4**a**) and substantiates the thesis that the perillaldehyde-mediated increase in lipid ROS starting form early time points is linked to ferroptosis. Indeed, lipid oxidative stress is a distinctive signature of ferroptotic cell death and never happens during other forms of regulated cell death, such as apoptosis, necroptosis or pyroptosis [34].

Lipid-ROS imbalance can be triggered by several mechanisms: (i) inhibition of the glutamate/cysteine Xc- anti-port system, which hampers the biosynthesis of intracellular GSH, (ii) depletion of intracellular GSH stores, or (iii) direct inhibition of the lipid repair enzyme GPX4, which requires GSH to counteract oxidative stress induced by lipid ROS [7,35]. Hence, among the inducers of ferroptosis, there are inhibitors that target Xc-, such as erastin, indicated as class 1 inducers, and/or inhibitors of GPX4 activity, such as RLS3, indicated as class 2 inducers. In addition, there are molecules that trigger ferroptosis by other mechanisms such as the accumulation of redox-active iron species or direct GSH depletion [36].

Perillaldehyde significantly decreased GPX4 expression in a time-dependent fashion (Fig. 4**b**). In particular, the expression of GPX4 was decreased by 2.7 times after 6 h and by 4.8 after 24 h compared to

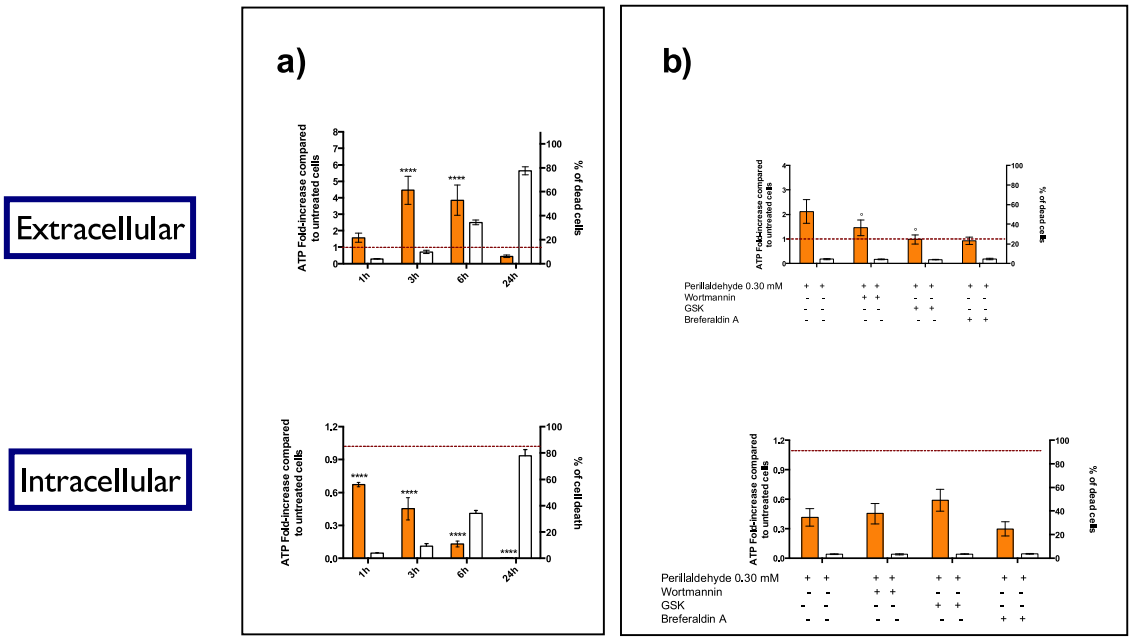

Fig. 5. Perillaldehyde induces active release of ATP. Time-dependent ATP emission into the medium (extracellular) or intracellular ATP content on HL-60 cells treated with perillaldehyde. (**a**) ATP emission into the medium (extracellular) or (**b**) intracellular ATP content on HL-60 cells pre-treated with wortmannin, GSK or brefaldin A for 1 h, then treated with perillaldehyde 0.30 mM for 3 h. The white bars represent the % of dead HL-60 cells, which corresponds to those cells with a broken membrane that would allow a passive secretion of ATP. The colored bars represent the ATP released into the extracellular medium or intracellularly. ATP is expressed as a fold increase compared to untreated cells. After 3 h, the amount of cell death was less than 10%, ATP extracellular release reaches the peak and intracellular ATP decreases in a time-dependent manner, suggesting that perillaldehyde promotes an active release of ATP. Statistical significance was calculated by two-way Anova followed by Dunnet's multiple comparisons test (**a**) or Uncorrected Fisher's LSD (**b**). * ** * $p < 0.0001$ compared to untreated cells. *$p < 0.05$ compared to HL-60 treated with no inhibitors and perillaldehyde 0.30 mM.

untreated cells from both perillaldehyde and RSL3 treatments (Fig. 4**b**).

The analysis of GPX4 expression is not sufficient to determine whether perillaldehyde increases lipid ROS through a direct or indirect inhibition of the enzyme. Since depletion of GSH represents another key mechanism favoring ferroptosis execution, as reported above, we analyzed the intracellular levels of GSH after treatment with perillaldehyde. We observed a time-dependent decrease in GSH levels at the same extent of the renowned ferroptosis inducer and system Xc- blocker, erastin (Fig. 4**c**). Both perillaldehyde and erastin depleted GSH in HL-60 cells by 50% after 6 h treatment at the highest tested concentrations.

Although further experiments will be necessary to define whether perillaldehyde is an Xc- system inhibitor (class 1) or a GPX4 inhibitor (class 2), these results confirmed that perillaldehyde induces ferroptosis.

3.4. *Perillaldehyde induces the active release of ATP*

The understanding of the interconnectivity of regulated cell death and innate/adaptative immunity has unearthed new opportunities to guide our immune system to beating cancer [37]. For example, apoptotic or necroptotic cells often possess immunogenic properties which can efficiently induce antitumor immunity through the so-called immunogenic cell death (ICD) [5]. ICD is a peculiar form of regulated cell death that promotes the activation of an adaptive immune response leading to the tumor eradication. When an ICD inducer kills tumor cells, it also provides the expression and presentation of tumor-associated antigens and the emission of the ICD mediators or adjuvants, such as cytokines and the damage-associated molecular patterns, or DAMPs, which promote the activation and maturation of dendritic cells and switch on the adaptive immunity engaging $CD8^+$ T lymphocytes [38–40]. One of the most peculiar DAMPs, which also represents a necessary condition for ICD execution, is the active secretion or passive release by dying cancer cells of ATP [38,39]. ATP represents a "find me signal" and, binding to the purinergic P_2X_7 receptors on dendritic cells, allows their activation and maturation. Moreover, the active release of ATP, compared to its passive secretion, provokes a better and more robust immune system stimulation [38,39,41]. Recently, we and others demonstrated that cancer cells dying by ferroptosis can as well stimulate the adaptative immune response [32,40,42]. This information prompted us to assess whether perillaldehyde could be a good ICD inducer candidate.

Thus, we monitored perillaldehyde's effect on ATP emission. We found that after 3 h of stimulation of HL-60 cells with perillaldehyde, the amount of cell death was less than just 10% while at the same time, the ATP extracellular release reaches the peak, suggesting that perillaldehyde promotes an active release of this DAMP (Fig. 5**a**). In parallel, intracellular ATP decreases in a time-dependent manner (Fig. 5**a**).

Indeed, DAMPs and cytokines emission must be tight regulated to induce a strong immunogenicity. For instance, it has been demonstrated that the optimal emission of ATP is mediated by autophagy [41]. In addition, Garg et al. [41] revealed that ATP active secretion is driven by endoplasmic reticulum (ER) stress in general and PKR-like endoplasmic reticulum kinase (PERK) activation in particular. Also, they demonstrated that ATP exploits the ER-Golgi transport pathway to be actively secreted and be able to interact with dendritic cells. Therefore, to confirm that the release of ATP was active, we monitored its release after 3 h treatment with the inhibitors of different pathways commonly involved in the active secretion of ATP [41,43–46]. We used GSK as a PERK inhibitor, wortmannin to block phosphoinositide 3-kinase (PI3K), and brefeldin A to stop protein secretion and the traffic between ER and Golgi. All the inhibitors almost completely restored physiological ATP extracellular levels while leaving unchanged intracellular levels (Fig. 5**b**), precisely as happens for hypericin-based photodynamic therapy, one of the most potent apoptotic ICD inducers known so far [41]. These data demonstrate that perillaldehyde promotes an active secretion of ATP, show ER stress involvement, and indicate PI3K-ER-Golgi as a route for secretion, exactly as the most potent ICD inducers [41]. These

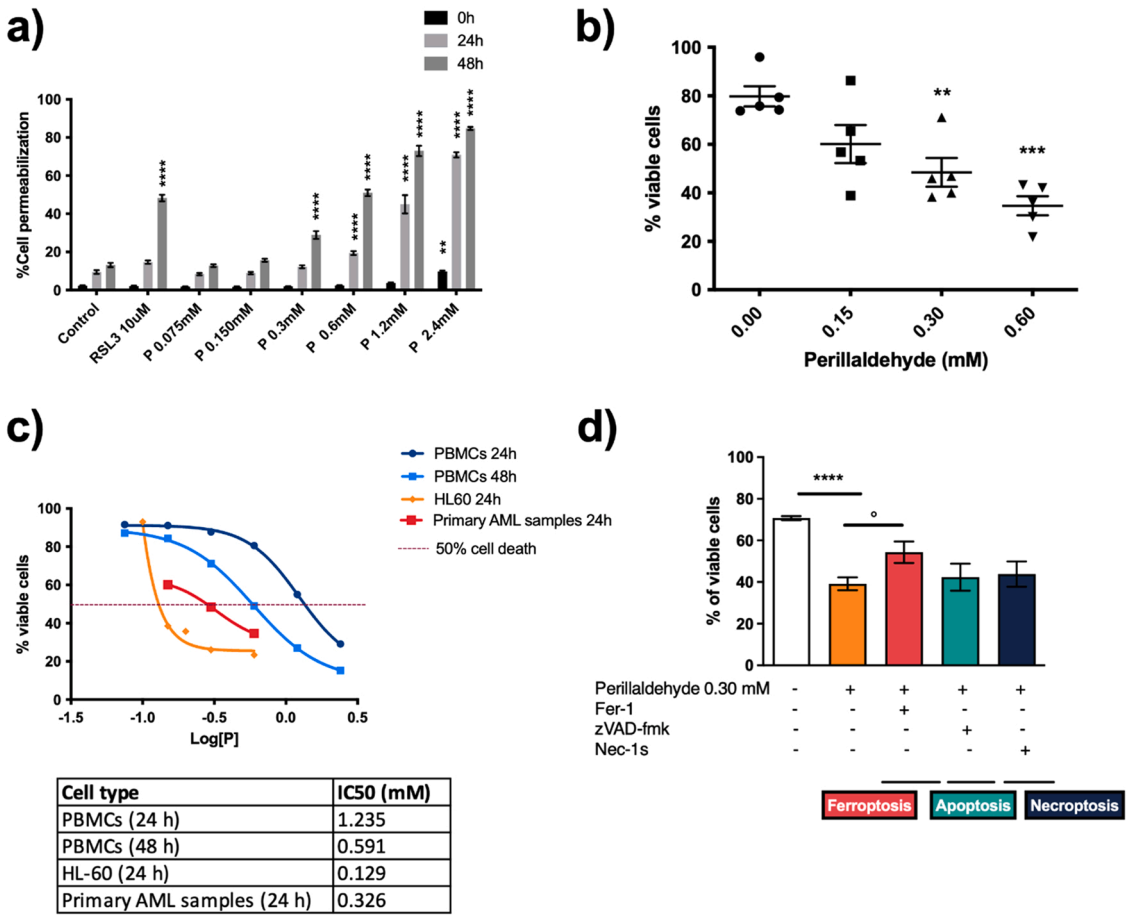

Cell type	IC50 (mM)
PBMCs (24 h)	1.235
PBMCs (48 h)	0.591
HL-60 (24 h)	0.129
Primary AML samples (24 h)	0.326

Fig. 6. Perillaldehyde is partially selective towards cancer cells and induces ferroptosis on samples obtained from AML patients. (**a**) PBMCs obtained from 4 different healthy volunteers were stimulated with perillaldehyde for 0, 24, and 48 h. Sytox Green was used as viability dye. (**b**) Cytotoxic effects of perillaldehyde after 24 h treatment of samples obtained from 5 AML patients stained with Sytox Blue. (**c**) Non-linear transformation of the % of viable cells and IC_{50} values on PBMCs treated with perillaldehyde for 24 or 48 h, HL-60 treated for 24 h or primary AML samples treated for 24 h with increasing concentrations of perillaldehyde. IC_{50} was calculated through non-linear regression. Perillaldehyde exerts cytotoxic effects with the following potency: HL60 > primary AML samples > PBMCs. (d) % of viable cells after 1 h pre-treatment of primary AML samples with inhibitors and treatment for 24 h with perillaldehyde 0.30 mM. Cell death was significantly reduced by the ferroptosis inhibitor fer-1, whereas inhibitors of apoptosis or necroptosis were ineffective. The following concentrations of inhibitors were used: 25 μM zVAD-fmk, 20 μM nec-1s, 1 μM fer-1 and Sytox Blue was used as viability dye. * * $p < 0.01$; * ** $p < 0.001$; * *** * $p < 0.0001$ compared to untreated cells. ° $p < 0.05$ compared to cells treated with perillaldehyde. Statistical significance was calculated by one-way Anova followed by Dunnet's multiple comparisons test (a, b) or Uncorrected Fisher's LSD (d).

data indicate for the first time that during ferroptotic cell death ATP can be actively secreted and substantiates the possibility that perillaldehyde induced ferroptosis with ICD features.

3.5. *Perillaldehyde is partially selective towards cancer cells and induces ferroptosis on primary AML samples*

To evaluate the actual antitumor potential of a drug, it is necessary to draw a risk-benefit *ratio*, by correlating the toxicological and pharmacological profiles. Regarding the toxicological profile, it is important to remind that perillaldehyde is routinely used in the food and perfume industry. Thus, it is characterized by a favorable toxicological profile and the lack of mutagenic potential [47,48]. Since our study supports a potential use of perillaldehyde in the oncological field, we investigated perillaldehyde's selectivity of action towards tumor cells. We exploited PBMCs extracted from 4 healthy volunteers. Perillaldehyde induced a concentration- and time-dependent cytotoxic effect on PBMCs, but it showed a lower potency on PBMCs compared to the effect on tumor cells. After 24 h, the IC_{50} recorded on PBMCs was almost 10 times higher than that recorded on HL-60. After 48 h, the IC_{50} recorded on PBMCs was still 5 times higher than that recorded on HL-60 still at 24 h (Fig. 6**a** and **d**). These results show a partial selectivity of action towards tumor cells and support the thesis of a favorable toxicological profile of perillaldehyde and point to its possible application in the clinical oncology.

The response to anticancer drugs can often vary from *in vitro* to *in vivo* studies and the lack of predictivity is often due to the simplified tumor cell line models that do not consider tumor heterogenicity. Even if key gene expression signatures are similar to *ex vivo* primary cells, tumor cell lines have poor biologic fidelity and poor sensitivity for patient-specific drug response. Indeed, they are homogeneous, derive from selected AML patients, acquire cytogenetic aberrations during the periods of cell culturing, *etc.* Primary AML samples reflect the bone marrow environment and can allow yielding representative results for anticancer drug testing [49]. If an anticancer drug results ineffective when patient tumor cells are directly exposed to the drug, it is unlikely to exhibit effect *in vivo* [50].

For this reason, we tested perillaldehyde on primary samples obtained from 5 AML patients. Perillaldehyde induced a concentration-dependent decrease in cell viability on all primary samples and at the same concentrations used in the *in vitro* test (Fig. 6**b**). It is interesting to notice that although the IC_{50} obtained on patients' samples (0.326 mM) is 2.5 higher than that recorded on HL-60 (0.129 mM), it is still 3.8 times lower than that recorded on PBMCs (1.235 mM), confirming the antitumor activity and the partial selectivity of action of this compound

(Fig. 6**c**).

To complete the study, we analyzed whether perillaldehyde induced ferroptosis in the primary samples from AML patients. For this reason, we repeated the cell death inhibitors assay and found that only fer-1, a ferroptosis inhibitor, restored cell viability (Fig. 6**d**), thus confirming the induction of ferroptosis by perillaldehyde recorded in HL-60 cell line.

4. Conclusions

AML is the most common type of acute leukemia in adults and remains a high risk disease with low cure rates despite intensive standard chemotherapy regimens [51], further decreasing with older age. In the past decades, research efforts focused on targeted therapy, mainly obtaining favorable results only for specific subsets of patients harboring particular genetic characteristics and, due the problem of resistance and relapses, providing only transient antileukemic responses in a high percentage of patients [52,53].

Ferroptosis induction is an emerging strategy in the oncological field, probably useful also to fight AML [54]. Although research about ferroptosis and AML is at an embryonic stage, that little knowledge hints to ferroptosis as an effective approach. For instance, the semi-synthetic antimalaria dihydroartemisinin and the flavonoid typhaneoside both demonstrated their ability to promote autophagy-dependent ferroptosis on AML cells while having a favorable toxicological profile [55,56]. Besides, an *in vitro* study demonstrated that the well-known ferroptosis inducer erastin showed interesting antileukemic activity, also increasing the sensitivity to conventional chemotherapy [57]. More recently, a publication disclosed that the new promising antileukemic agent APR-246, a first-in-class mutant p53 reactivator, triggered AML ferroptotic cell death through intracellular GSH depletion. GSH depletion was due to the modulation of the SLC7A11 subunit of the cystine/glutamate antiporter [58]. A phase one clinical study also showed its safety profile on AML patients in combination with the hypomethylating agent azacitidine [59].

All this evidence points to the potential pharmacological usefulness of ferroptosis in the treatment of AML and the antileukemic activity of perillaldehyde reported in this paper perfectly fits this context. Here, we demonstrated that R-perillaldehyde, the main component of the essential oil of *A. leucotrichus*, promotes ferroptosis on two leukemia cell lines and on primary AML samples obtained from patients, and showed low toxicity on normal cells, exhibiting a favorable risk-benefit profile. Furthermore, it promoted the active secretion of ATP, which is one of the most crucial events in ICD, qualifying itself for further studies to disclose its actual antitumor-immunogenic potential. Overall, these data depict a very favorable and peculiar antileukemic profile of perillaldehyde and qualify this natural product to proceed further through the drug development pipeline, starting with *in vivo* studies.

CRediT authorship contribution statement

Carmela Fimognari and Dmitri V. Krysko conceived the idea and supervised the study. Elena Catanzaro, Eleonora Turrini, Tessa Kerre, Simon Sioen, Ans Baeyens, Alessandra Guerrini, Mohamed Lamin Abdi Bellau, carried out the experiments and performed data analysis. Elena Catanzaro, Eleonora Turrini, Tessa Kerre, Simon Sioen, Ans Baeyens and Alessandra Guerrini wrote the draft. Carmela Fimognari, Dmitri Krysko, Gianni Sacchetti, Alessandra Guerrini and Guglielmo Paganetto reviewed the draft. All authors have approved the final article.

Declaration of Competing Interest

The authors declare that they have no known competing financial interests or personal relationships that could have appeared to influence the work reported in this paper.

Acknowledgments

This study is partially supported by FIR2016 grant of the University of Ferrara to A.G. and FFABR 2017-MIUR to A.G. D.V.K. lab is supported by FWO-Flanders (G043219N, FWO G016221), Ghent University BOF (Special Research Fund 01/O3618 and BOF/IOP/2022/033) and the project (40007488) from the FWO and F.R.S.-FNRS under the "Excellence of Science" program. The funding sources were not involved in study design; in the collection, analysis and interpretation of data; in the writing of the report; and in the decision to submit the article for publication. The authors are grateful to the Sahrawi Ministry of Public Health, Omar Mih, representative of Polisario Front in Italy. We also thank prof. Marco Fogagnolo for GC-FID experiments.

Appendix A. Supporting information

Supplementary data associated with this article can be found in the online version at doi:10.1016/j.biopha.2022.113662.

References

[1] Y. Fuchs, H. Steller, Programmed cell death in animal development and disease, Cell 147 (4) (2011) 742–758, https://doi.org/10.1016/j.cell.2011.10.033.
[2] L. Galluzzi, I. Vitale, S.A. Aaronson, J.M. Abrams, D. Adam, P. Agostinis, et al., Molecular mechanisms of cell death: recommendations of the Nomenclature Committee on Cell Death 2018, Cell Death Differ. 25 (3) (2018) 486–541, https://doi.org/10.1038/s41418-017-0012-4.
[3] R.M. Mohammad, I. Muqbil, L. Lowe, C. Yedjou, H.-Y. Hsu, L.-T. Lin, et al., Broad targeting of resistance to apoptosis in cancer, Semin Cancer Biol. 35 (2015) S78–S103, https://doi.org/10.1016/j.semcancer.2015.03.001.
[4] S.W.G. Tait, G. Ichim, D.R. Green, Die another way–non-apoptotic mechanisms of cell death, J. Cell Sci. 127 (Pt 10) (2014) 2135–2144, https://doi.org/10.1242/jcs.093575.
[5] O. Krysko, T.L. Aaes, V.E. Kagan, K. D'Herde, C. Bachert, L. Leybaert, et al., Necroptotic cell death in anti-cancer therapy, Immunol. Rev. 280 (1) (2017) 207–219, https://doi.org/10.1111/imr.12583.
[6] S.J. Dixon, K.M. Lemberg, M.R. Lamprecht, R. Skouta, E.M. Zaitsev, C.E. Gleason, et al., Ferroptosis: an iron-dependent form of nonapoptotic cell death, Cell 149 (5) (2012) 1060–1072, https://doi.org/10.1016/j.cell.2012.03.042.
[7] E. Dierge, E. Debock, C. Guilbaud, C. Corbet, E. Mignolet, L. Mignard, et al., Peroxidation of n-3 and n-6 polyunsaturated fatty acids in the acidic tumor environment leads to ferroptosis-mediated anticancer effects, e5, Cell Metab. 33 (8) (2021) 1701–1715, https://doi.org/10.1016/j.cmet.2021.05.016.
[8] D.J. Newman, G.M. Cragg, Natural products as sources of new drugs over the nearly four decades from 01/1981 to 09/2019, J. Nat. Prod. 83 (3) (2020) 770–803, https://doi.org/10.1021/acs.jnatprod.9b01285.
[9] C. Fimognari, L. Ferruzzi, E. Turrini, G. Carulli, M. Lenzi, P. Hrelia, et al., Metabolic and toxicological considerations of botanicals in anticancer therapy, Expert Opin. Drug Metab. Toxicol. 8 (7) (2012) 819–832, https://doi.org/10.1517/17425255.2012.685717.
[10] G. Greco, E. Catanzaro, C. Fimognari, Natural products as inducers of non-canonical cell death: a weapon against cancer, Cancers 13 (2) (2021) 304, https://doi.org/10.3390/cancers13020304.
[11] E. Idm'hand, F. Msanda, K. Cherifi, Medicinal uses, phytochemistry and pharmacology of Ammodaucus leucotrichus, Clin. Phytoscience 6 (1) (2020) 6, https://doi.org/10.1186/s40816-020-0154-7.
[12] I.A. El-Haci, C. Bekhechi, F. Atik-Bekkara, W. Mazari, M. Gherib, A. Bighelli, et al., Antimicrobial activity of Ammodaucus leucotrichus fruit oil from Algerian Sahara, Nat. Prod. Commun. 9 (5) (2014) 711–712.
[13] A. Khaldi, B. Meddah, A. Moussaoui, P. Sonnet, Anti-mycotoxin effect and antifungal properties of essential oil from ammodaucus leucotrichus Coss. & Dur. on Aspergillus flavus and Aspergillus ochraceus, J. Essent. Oil Bear. Plants 20 (1) (2017) 36–44, https://doi.org/10.1080/0972060X.2017.1282840.
[14] D. Dahmane, T. Dob, S. Krimat, A. Nouasri, H. Metidji, A. Ksouri, Chemical composition, antioxidant and antibacterial activities of the essential oils of medicinal plant Ammodaucus leucotrichus from Algeria, J. Essent. Oil Res. 29 (1) (2017) 48–55, https://doi.org/10.1080/10412905.2016.1201015.
[15] N. Sadaoui, N. Bec, V. Barragan-Montero, N. Kadri, F. Cuisinier, C. Larroque, et al., The essential oil of Algerian Ammodaucus leucotrichus Coss. & Dur. and its effect on the cholinesterase and monoamine oxidase activities, Fitoterapia 130 (2018) 1–5, https://doi.org/10.1016/j.fitote.2018.07.015.
[16] M. Khalfaoui, F. Chebrouk, B.E.C. Ziani, N. Bennamane, B. Cherfaoui, W. Frites, et al., Hemi-synthesis, in-vitro and in-silico bioactivities of new chiral-Schiff bases and benzodiazepine derivatives from Ammodaucus leucotrichus(S)-perillaldehyde, J. Mol. Struct. 1241 (2021), 130690, https://doi.org/10.1016/j.molstruc.2021.130690.
[17] H. Mohammedi, S. Idjeri-Mecherara, F. Menaceur, K. Azine, A. Hassani, Chemical compositions of extracted volatile oils of ammodaucus leucotrichus L. Fruit from different geographical regions of algeria with evaluation of its toxicity, anti-

inflammatory and antimicrobial activities, J. Essent. Oil Bear. Plants 21 (6) (2018) 1568–1584, https://doi.org/10.1080/0972060X.2018.1559102.
[18] M. Zielińska-Błajet, P. Pietrusiak, J. Feder-Kubis, Selected monocyclic monoterpenes and their derivatives as effective anticancer therapeutic agents, Int. J. Mol. Sci. 22 (9) (2021) 4763, https://doi.org/10.3390/ijms22094763.
[19] J. Tian, X. Zeng, A. Lü, A. Zhu, X. Peng, Y. Wang, Perillaldehyde, a potential preservative agent in foods: Assessment of antifungal activity against microbial spoilage of cherry tomatoes, LWT - Food Sci. Technol. 60 (1) (2015) 63–70, https://doi.org/10.1016/j.lwt.2014.08.014.
[20] J.A. Elegbede, R. Flores, R.C. Wang, Perillyl alcohol and perillaldehyde induced cell cycle arrest and cell death in BroTo and A549 cells cultured in vitro, Life Sci. 73 (22) (2003) 2831–2840, https://doi.org/10.1016/s0024-3205(03)00701-x.
[21] Y. Zhang, S. Liu, Q. Feng, X. Huang, X. Wang, Y. Peng, et al., Perilaldehyde activates AMP-activated protein kinase to suppress the growth of gastric cancer via induction of autophagy, J. Cell Biochem (2018), https://doi.org/10.1002/jcb.27491.
[22] Z. Lin, S. Huang, X. LingHu, Y. Wang, B. Wang, S. Zhong, et al., Perillaldehyde inhibits bone metastasis and receptor activator of nuclear factor-κB ligand (RANKL) signaling-induced osteoclastogenesis in prostate cancer cell lines, Bioengineered 13 (2) (2022) 2710–2719, https://doi.org/10.1080/21655979.2021.2001237.
[23] L.N. Andrade, T.C. Lima, R.G. Amaral, C.D.Ó. Pessoa, M.O. Filho, M. de, B. M. Soares, et al., Evaluation of the cytotoxicity of structurally correlated p-menthane derivatives, Molecules 20 (7) (2015) 13264–13280, https://doi.org/10.3390/molecules200713264.
[24] E.B. Souto, S.B. Souto, A. Zielinska, A. Durazzo, M. Lucarini, A. Santini, et al., Perillaldehyde 1,2-epoxide loaded SLN-tailored mab: production, physicochemical characterization and in vitro cytotoxicity profile in MCF-7 cell lines, Pharmaceutics 12 (2) (2020) 161, https://doi.org/10.3390/pharmaceutics12020161.
[25] L.N. Andrade, P. Severino, R.G. Amaral, G.A.A. Doria, A. Silva, M. da., Alves, et al., Evaluation of cytotoxic and antitumor activity of perillaldehyde 1,2-epoxide, JMPR 12 (30) (2018) 590–600, https://doi.org/10.5897/JMPR2018.6699.
[26] Z. Hui, M. Zhang, L. Cong, M. Xia, J. Dong, Synthesis and antiproliferative effects of amino-modified perillyl alcohol derivatives, Molecules 19 (5) (2014) 6671–6682, https://doi.org/10.3390/molecules19056671.
[27] R. Demuynck, I. Efimova, A. Lin, H. Declercq, D.V. Krysko, A 3D cell death assay to quantitatively determine ferroptosis in spheroids, Cells 9 (3) (2020), E703, https://doi.org/10.3390/cells9030703.
[28] I. Rahman, A. Kode, S.K. Biswas, Assay for quantitative determination of glutathione and glutathione disulfide levels using enzymatic recycling method, Nat. Protoc. 1 (6) (2006) 3159–3165, https://doi.org/10.1038/nprot.2006.378.
[29] V.D. Turubanova, I.V. Balalaeva, T.A. Mishchenko, E. Catanzaro, R. Alzeibak, N. N. Peskova, et al., Immunogenic cell death induced by a new photodynamic therapy based on photosens and photodithazine, J. Immunother. Cancer 7 (1) (2019) 350, https://doi.org/10.1186/s40425-019-0826-3.
[30] R.P. Adams, Identification of Essential Oil Components by Gas Chromatography/mass Spectrometry, Allured Publishing Corporation, 2007.
[31] I. Shlomovitz, M. Speir, M. Gerlic, Flipping the dogma – phosphatidylserine in non-apoptotic cell death, Cell Commun. Signal 17 (1) (2019) 139, https://doi.org/10.1186/s12964-019-0437-0.
[32] I. Efimova, E. Catanzaro, L. Van der Meeren, V.D. Turubanova, H. Hammad, T. A. Mishchenko, et al., Vaccination with early ferroptotic cancer cells induces efficient antitumor immunity, J. Immunother. Cancer 8 (2) (2020), e001369, https://doi.org/10.1136/jitc-2020-001369.
[33] S. Zargarian, I. Shlomovitz, Z. Erlich, A. Hourizadeh, Y. Ofir-Birin, B.A. Croker, et al., Phosphatidylserine externalization, "necroptotic bodies" release, and phagocytosis during necroptosis, PLoS Biol. 15 (6) (2017), e2002711, https://doi.org/10.1371/journal.pbio.2002711.
[34] B. Wiernicki, H. Dubois, Y.Y. Tyurina, B. Hassannia, H. Bayir, V.E. Kagan, et al., Excessive phospholipid peroxidation distinguishes ferroptosis from other cell death modes including pyroptosis, Cell Death Dis. 11 (10) (2020) 1–11, https://doi.org/10.1038/s41419-020-03118-0.
[35] W.S. Yang, B.R. Stockwell, Ferroptosis: death by lipid peroxidation, Trends Cell Biol. 26 (3) (2016) 165–176, https://doi.org/10.1016/j.tcb.2015.10.014.
[36] S. Zuo, J. Yu, H. Pan, L. Lu, Novel insights on targeting ferroptosis in cancer therapy, Biomark. Res. 8 (1) (2020) 50, https://doi.org/10.1186/s40364-020-00229-w.
[37] A.J. Legrand, M. Konstantinou, E.F. Goode, P. Meier, The diversification of cell death and immunity: memento mori, Mol. Cell 76 (2) (2019) 232–242, https://doi.org/10.1016/j.molcel.2019.09.006.
[38] J. Fucikova, O. Kepp, L. Kasikova, G. Petroni, T. Yamazaki, P. Liu, et al., Detection of immunogenic cell death and its relevance for cancer therapy, Cell Death Dis. 11 (11) (2020) 1–13, https://doi.org/10.1038/s41419-020-03221-2.
[39] L. Galluzzi, I. Vitale, S. Warren, S. Adjemian, P. Agostinis, A.B. Martinez, et al., Consensus guidelines for the definition, detection and interpretation of immunogenic cell death, J. Immunother. Cancer 8 (1) (2020), e000337, https://doi.org/10.1136/jitc-2019-000337.
[40] R. Demuynck, I. Efimova, F. Naessens, D.V. Krysko, Immunogenic ferroptosis and where to find it? J. Immunother. Cancer 9 (12) (2021), e003430 https://doi.org/10.1136/jitc-2021-003430.
[41] A.D. Garg, D.V. Krysko, T. Verfaillie, A. Kaczmarek, G.B. Ferreira, T. Marysael, et al., A novel pathway combining calreticulin exposure and ATP secretion in immunogenic cancer cell death, EMBO J. 31 (5) (2012) 1062–1079, https://doi.org/10.1038/emboj.2011.497.
[42] J. Liu, S. Zhu, L. Zeng, J. Li, D.J. Klionsky, G. Kroemer, et al., DCN released from ferroptotic cells ignites AGER-dependent immune responses, Autophagy (2021) 1–14, https://doi.org/10.1080/15548627.2021.2008692.
[43] D. D'Eliseo, L. Manzi, F. Velotti, Capsaicin as an inducer of damage-associated molecular patterns (DAMPs) of immunogenic cell death (ICD) in human bladder cancer cells, Cell Stress Chaperon-.-. 18 (6) (2013) 801–808, https://doi.org/10.1007/s12192-013-0422-2.
[44] L. Galluzzi, O. Kepp, G. Kroemer, Enlightening the impact of immunogenic cell death in photodynamic cancer therapy, EMBO J. 31 (5) (2012) 1055–1057, https://doi.org/10.1038/emboj.2012.2.
[45] X. Li, J. Zheng, S. Chen, F.-D. Meng, J. Ning, S.-L. Sun, Oleandrin, a cardiac glycoside, induces immunogenic cell death via the PERK/elF2α/ATF4/CHOP pathway in breast cancer, Cell Death Dis. 12 (4) (2021) 314, https://doi.org/10.1038/s41419-021-03605-y.
[46] L.C. Gomes-da-Silva, L. Zhao, L. Bezu, H. Zhou, A. Sauvat, P. Liu, et al., Photodynamic therapy with redaporfin targets the endoplasmic reticulum and Golgi apparatus, EMBO J. 37 (13) (2018), e98354, https://doi.org/10.15252/embj.201798354.
[47] S.M. Cohen, S. Fukushima, N.J. Gooderham, F.P. Guengerich, S.S. Hecht, I.M.C. M. Rietjens, et al., FEMA expert panel review of p -mentha-1,8-dien-7-al genotoxicity testing results, Food Chem. Toxicol. 98 (2016) 201–209, https://doi.org/10.1016/j.fct.2016.10.020.
[48] C.A. Hobbs, S.V. Taylor, C. Beevers, M. Lloyd, R. Bowen, L. Lillford, et al., Genotoxicity assessment of the flavouring agent, perillaldehyde, Food Chem. Toxicol. 97 (2016) 232–242, https://doi.org/10.1016/j.fct.2016.08.029.
[49] D.G.J. Cucchi, R.W.J. Groen, J.J.W.M. Janssen, J. Cloos, Ex vivo cultures and drug testing of primary acute myeloid leukemia samples: Current techniques and implications for experimental design and outcome, Drug Resist. Updates 53 (2020), 100730, https://doi.org/10.1016/j.drup.2020.100730.
[50] K. Blom, P. Nygren, J. Alvarsson, R. Larsson, C.R. Andersson, Ex vivo assessment of drug activity in patient tumor cells as a basis for tailored cancer therapy, J. Lab Autom. 21 (1) (2016) 178–187, https://doi.org/10.1177/2211068215598117.
[51] M. Stanchina, D. Soong, B. Zheng-Lin, J.M. Watts, J. Taylor, Advances in acute myeloid leukemia: recently approved therapies and drugs in development, Cancers 12 (11) (2020) 3225, https://doi.org/10.3390/cancers12113225.
[52] A.B. Kagan, B.S. Moses, B.T. Mott, G. Rai, N.M. Anders, M.A. Rudek, et al., A novel 2-carbon-linked dimeric artemisinin with potent antileukemic activity and favorable pharmacology, Front. Oncol. (2022) **11**.
[53] S. Scholl, M. Fleischmann, U. Schnetzke, F.H. Heidel, Molecular mechanisms of resistance to FLT3 inhibitors in acute myeloid leukemia: ongoing challenges and future treatments, Cells 9 (11) (2020), E2493, https://doi.org/10.3390/cells9112493.
[54] Y. Zou, M.J. Palte, A.A. Deik, H. Li, J.K. Eaton, W. Wang, et al., A GPX4-dependent cancer cell state underlies the clear-cell morphology and confers sensitivity to ferroptosis, Nat. Commun. 10 (1) (2019) 1617, https://doi.org/10.1038/s41467-019-09277-9.
[55] J. Du, T. Wang, Y. Li, Y. Zhou, X. Wang, X. Yu, et al., DHA inhibits proliferation and induces ferroptosis of leukemia cells through autophagy dependent degradation of ferritin, Free Radic. Biol. Med 131 (2019) 356–369, https://doi.org/10.1016/j.freeradbiomed.2018.12.011.
[56] H.-Y. Zhu, Z.-X. Huang, G.-Q. Chen, F. Sheng, Y.-S. Zheng, Typhaneoside prevents acute myeloid leukemia (AML) through suppressing proliferation and inducing ferroptosis associated with autophagy, Biochem Biophys. Res Commun. 516 (4) (2019) 1265–1271, https://doi.org/10.1016/j.bbrc.2019.06.070.
[57] Y. Yu, Y. Xie, L. Cao, L. Yang, M. Yang, M.T. Lotze, et al., The ferroptosis inducer erastin enhances sensitivity of acute myeloid leukemia cells to chemotherapeutic agents, Mol. Cell Oncol. 2 (4) (2015), https://doi.org/10.1080/23723556.2015.1054549.
[58] R. Birsen, C. Larrue, J. Decroocq, N. Johnson, N. Guiraud, M. Gotanegre, et al., APR-246 induces early cell death by ferroptosis in acute myeloid leukemia, Haematologica 107 (2) (2022) 403–416, https://doi.org/10.3324/haematol.2020.259531.
[59] D.A. Sallman, A.E. DeZern, G. Garcia-Manero, D.P. Steensma, G.J. Roboz, M. A. Sekeres, et al., Eprenetapopt (APR-246) and azacitidine in TP53-mutant myelodysplastic syndromes, JCO 39 (14) (2021) 1584–1594, https://doi.org/10.1200/JCO.20.02341.